

AD-A091 624

ROYAL AIRCRAFT ESTABLISHMENT FARNBOROUGH (ENGLAND)
THE PREDICTION OF THE BURSTING OF LAMINAR SEPARATION BUBBLES IN--ETC(U)
MAY 80 B R WILLIAMS

F/G 20/4

UNCLASSIFIED

RAE-TR-80060

ORIC-BR-74909

NL

1 1 1
AL
208-1



END
DATE
FILMED
12 80
DTIC

AD A091624



ROYAL AIRCRAFT ESTABLISHMENT

Technical Report 2090

May 1980

**THE PREDICTION OF THE BURSTING OF
LAMINAR SEPARATION BUBBLES IN THE
DESIGN OF TWO-DIMENSIONAL
HIGH-LIFT AEROFOILS**

By

B.R. Williams

RTIC
S-100

Prepared by

Personnel of



ROYAL AIRCRAFT ESTABLISHMENT

⑨ Technical Report 80060

Received for printing 1 May 1980

⑪ MS-7 80

THE PREDICTION OF THE BURSTING OF LAMINAR SEPARATION BUBBLES IN THE DESIGN OF TWO-DIMENSIONAL HIGH-LIFT AEROFOILS.

by

⑩ B. R. Williams

⑭ PHE-TR-89967

SUMMARY

→ The structure of laminar separation bubbles is described and methods of predicting the bursting of these bubbles on the slat of a high-lift wing are examined. In particular Horton's method is found to give a useful description of the growth and bursting of the bubble. A simple method of predicting the burst of short bubbles is developed by combining the Crabtree maximum pressure rise parameter with the assumption that the separated turbulent shear layer is an equilibrium flow. These methods will aid the design of wind-tunnel models and form one of the building blocks for the calculation of the viscous flow about high-lift wings.

Departmental Reference: Aero 3479 ✓

Copyright
©
Controller HMSO London
1980

310450

JOB

LIST OF CONTENTS

	<u>Page</u>
1 INTRODUCTION	3
2 STRUCTURE OF A LAMINAR SEPARATION BUBBLE	4
3 PREDICTION OF BUBBLE GROWTH FOR HIGH-LIFT AEROFOILS	5
4 PREDICTION FOR A SINGLE AEROFOIL	7
4.1 NACA 63-009 aerofoil section	7
4.2 12.2% thick RAE 100 aerofoil section	8
5 ALTERNATIVE PREDICTION METHODS	10
6 CONCLUSIONS	12
Tables 1 and 2	14
List of symbols	15
References	16
Illustrations	Figures 1-20
Report documentation page	inside back cover

Accession For	
NTIS GRA&I	<input checked="" type="checkbox"/>
DDC TAB	<input type="checkbox"/>
Unannounced	<input type="checkbox"/>
Justification	<input type="checkbox"/>
By _____	
Distribution/ _____	
Availability Codes	
Dist	Avail and/or special
A	

1 INTRODUCTION

The large pressure rises, which occur on multiple-element wings developing high-lift coefficients, can lead to the formation of laminar separation bubbles, particularly at the Reynolds numbers of wind-tunnel tests: the bursting of the bubble can determine the maximum lift on the wing. The formation, growth and bursting of the laminar separation bubble are strongly dependent on the Reynolds number and are usually associated with the Reynolds number obtained in atmospheric wind tunnels rather than those associated with full scale. The extrapolation from wind-tunnel results to full scale can thus be difficult, if not impossible. In the design of models for wind-tunnel testing a method of predicting the existence and possible bursting of the bubble is required so that it can be ensured that the flow is similar at test and full scale Reynolds number. In the new RAE 5m tunnel, tests can be performed at up to three atmospheres total pressure giving a range of Reynolds numbers which in some cases extend to full scale. In tests performed at different Reynolds numbers a bubble may burst at low Reynolds number, provoking a stall, whilst at high Reynolds number the flow will remain attached at the same incidence. As the loading increases with pressurisation (*ie* with increasing Reynolds number) it is important that this change in the flow can be predicted so that models of sufficient strength can be designed. The ability to predict the growth and bursting of laminar separation bubbles is examined in this Report and it is shown that the trends are well-predicted by the method due to Horton¹.

The prediction of the behaviour of the bubble is most crucial in the design of the slat of a high-lift model. The application of Horton's approach to these flows must be treated with some caution as the pressure gradients on the slat are much larger than those used in the development of the method. Horton's method and several other parametric descriptions of bubbles are checked against three sets of results taken from recent wind-tunnel tests. The examples to be considered are taken from tests on three models: a swept 'tapered' half-model, a constant chord swept 'panel' half-model and an 'end-plate' model. All the models have the same normalised section and are illustrated in Figs 1 and 2. The tapered and panel models exhibit a marked slat leading-edge stall, whilst the end-plate model stalls from the trailing edge of the wing. It is found that the parametric descriptions of the bubble are ambiguous; a slight change to Horton's method however leads to good agreement with the experimental behaviour.

Wood² reported that Horton's method failed to predict the development of the laminar bubble on a NACA 63-009 single aerofoil. This failure is explained

and corrected by comparing the method with results of a two-dimensional experiment³ on a 12.2% thick RAE 100 section; the stall on this section changes from leading-edge type to trailing-edge type as the Reynolds number is increased from 0.55×10^6 to 1.78×10^6 . Horton's method predicts the physical extent of the bubble and the change in stall behaviour with increased Reynolds number.

In the last section a simple method of predicting a bubble burst is developed by combining the Crabtree maximum pressure rise parameter with the assumption that the separated turbulent shear layer is an equilibrium flow.

2 STRUCTURE OF A LAMINAR SEPARATION BUBBLE

The development of a 'short bubble', which does not appreciably affect the external flow, can be divided into two regions. In the first region the separated viscous shear layer is laminar and there is a region of constant pressure on the surface. In the second region, transition to a turbulent layer is followed by entrainment of fluid into the turbulent layer; this entrainment process leads to the reattachment of the layer.

Owen and Klanfer⁴ characterised short bubbles by the Reynolds number based on the displacement thickness of the layer at separation $(R_{\delta_1})_s$. For short bubbles observations show that $(R_{\delta_1})_s$ is greater than 450, whilst 'long bubbles' (*ie* those significantly altering the external flow) are associated with values of $(R_{\delta_1})_s$ less than 450. If the adverse pressure gradient is too steep then the turbulent layer does not reattach and the bubble bursts; the separated shear layer then merges into the wake.

Crabtree⁵ observed that there is not in fact a unique value of $(R_{\delta_1})_s$ which can be used to predict the change from a short bubble to a bubble burst (or a long bubble). This is illustrated here by calculating the development of the laminar boundary layer through the pressure distributions measured on the slats of the three wind-tunnel models. The boundary layer is examined at conditions where on the tapered and panel models there is a change from a short bubble to a burst bubble whereas on the end plate model a bubble-burst does not occur. From the Owen and Klanfer criterion it might be expected that $(R_{\delta_1})_s$ would decrease through the value of 450 on the tapered and panel models.

The development of the laminar boundary layer is calculated by the method due to Thwaites⁶ and the values of $(R_{\delta_1})_s$ are given in Table 1. For the tapered model, calculations have been made for a section at 60% semi-span at α_1 (incidence 22.6°) and α_2 (22.8°); the bubble is known to burst at a slightly higher incidence. It is difficult in an experiment to obtain

sufficient measurements of the pressure on the slat to give a reliable calculation of the development of the boundary layer. For the α_2 incidence on the tapered model extra points have been interpolated in the pressure distribution to give more accurate results; the change induced by returning to the number of points used in the experiment is examined later in this section. In an attempt to investigate the situation that would exist if the bubble had not burst, the pressure distribution at α_3 (23°) is constructed by a linear extrapolation from α_1 and α_2 . As Table 1 shows the calculated value of $(R_{\delta_1})_s$ does not approach the critical value of 450. A value of $(R_{\delta_1})_s$ well above 450 is also obtained for the slat of the panel model which is just below an incidence at which bursting is observed. The slat on the end-plate model, which does not exhibit a bubble burst, produces a value of $(R_{\delta_1})_s$ which is comparable to the values for the other two models. These calculations thus support Crabtree's conclusion that the Owen and Klanfer criterion is unable to predict the change from short to long bubbles.

The physical basis of the Owen and Klanfer criterion is considered to be that, in a flat plate boundary layer, turbulent spots do not grow for $R_{\delta_1} < 450$. For a bubble with $(R_{\delta_1})_s > 450$ the growth of the turbulent spots will cause a rapid transition to a turbulent layer thus enabling the layer to reattach and form a short bubble. Crabtree indicated that the pressure attainable by the reattaching layer is also an important parameter for distinguishing bubbles. He defined $\sigma = (Cp_r - Cp_s)/(1 - Cp_s)$ where s and r refer to separation and reattachment respectively. Experimentally it was found that as the bubble approached the bursting point σ reached a maximum value of 0.35. In section 5 it is assumed that the separated turbulent shear layer is an equilibrium flow: this permits a simple integration of the shear layer equations which, combined with the Crabtree parameter, gives a simple bursting criterion.

3 PREDICTION OF BUBBLE GROWTH FOR HIGH-LIFT AEROFOILS

The production of a semi-empirical theory for the growth of laminar separation bubbles by Horton enabled the point of reattachment to be determined. A short summary of Horton's method is followed by an examination of its ability to predict the form of the bubble on the slats of the three models. Once the point of reattachment is known, Crabtree's parameter σ can be calculated and it is shown that σ is close to its maximum value for bubbles which Horton's method indicates are close to bursting.

Since the processes governing the transition of viscous shear layers are not well understood, Horton took the length of the laminar bubble, l_1 , from an

experimental correlation. Owen and Klanfer suggested that $(R_{\delta_1})_s$ is an important parameter determining λ_1 . $(R_{\delta_1})_s$ is proportional to the Reynolds number based on the momentum thickness at separation, $(R_{\theta})_s$ and in Fig 3 a band covering the values of λ_1 from some 40 experiments is plotted against $(R_{\theta})_s$.

Horton concludes that the relationship

$$\frac{\lambda_1}{\theta_s} = \frac{c \times 10^4}{R_{\theta_s}}, \quad (1)$$

with $c = 4$, is an adequate description of these results. For the prediction of the development of the turbulent shear layer, Horton found that the reattachment process could be characterised by the parameter $\Lambda_R = [(\theta/u_e)(du_e/dx)]$ where u_e is the inviscid velocity outside the layer. Experimentally the value of the parameter for reattachment is found to be $\Lambda_R = -0.0082$. Horton assumed that the velocity varies linearly between transition and reattachment and using constant mean values for the energy thickness shape parameter and the dissipation coefficient, he integrated the energy equation of the turbulent layer to give a locus of possible reattachment positions in terms of the pressure coefficient and distance. Horton introduced two further empirical constants to give a complete description of the turbulent layer. Since short bubbles have only a local effect upon the pressure distribution it is assumed that the reattachment position is given by the intersection of the locus of possible reattachment positions with the pressure distribution. An example of this calculation for the slat of the tapered model at α_1 is given in Fig 4.

Calculations using the experimental pressure distributions with the length of the laminar bubble given by equation (1), with values of c of 4, 5 and 6, are illustrated in Figs 4 to 7. A bubble burst is indicated by the non-intersection of the locus and the pressure distribution and it can be seen that for $c = 4$ the tapered- and panel-model cases (Figs 4 to 6) are much closer to bursting than the endplate-model case (Fig 7). This corresponds to the experimental behaviour noted in the introduction. The sensitivity of the estimated position of reattachment to the assumed value of c is most evident in Fig 5 where for $c = 5$ the reattachment point is further downstream than for $c = 4$ and for $c = 6$ the turbulent layer fails to reattach and the bubble bursts. At α_2 the experimental bubble is on the point of bursting so for this case a value of $c = 5$ gives a better description of the growth of the bubble. The predictions with $c = 5$ given in Figs 4, 6 and 7 are also consistent with the observed behaviour.

The value of the Crabtree parameter, σ , is thus evaluated using the pressure coefficient at reattachment from Horton's method with $c = 5$. The results are given in Table 1 and for the tapered model at α_2 , σ is 0.34 which is close to the value for bursting of 0.35. For α_3 on the tapered model the value of σ is disappointingly low and this result is discussed in the next paragraph. It can be concluded that Horton's method closely approximates the physical process of the development and bursting of laminar separation bubbles. The maximum pressure-rise coefficient, σ , also predicts the bursting of the bubble.

These calculations are very sensitive to the shape of the pressure distribution and inaccuracies are introduced by the linear interpolation of the pressure distribution defined by only a few experimental points. The calculation for the tapered model at α_2 with the pressure distribution defined by only a few points is illustrated in Fig 8. The separation point has moved forward and by reference to Table 2 the value of σ is seen to be uncharacteristically low; all the usual parameters would suggest that the bubble is not close to bursting. However on closer examination of Fig 8, the locus of possible reattachment positions only just intersects the physical pressure distribution and this suggests that the bubble is on the point of bursting. An examination of the closeness of the locus of possible reattachment positions to the pressure distribution is a better guide to bubble bursting than the parameters of the bubble. On re-examination of the calculation with the extrapolated pressure distribution (α_3) for the tapered model the misleading values of the normal parameters are explained by the small number of points used to define the pressure distribution; in Fig 8 the locus of reattachment points is reasonably close to the pressure distribution indicating a bubble burst.

4 PREDICTION FOR A SINGLE AEROFOIL

4.1 NACA 63-009 aerofoil section

The work of Gault⁷ on the NACA 63-009 section forms one of the most detailed experimental studies of the structure of a laminar separation bubble and it is natural to use these results to test any theory on bubble growth. In an extensive parametric study Wood² found that the experimental characteristics of the bubble were not predicted by Horton's method. The study used inviscid pressure distributions and this will give poor agreement for at least two reasons. At comparable lift coefficients the viscous effects increase the loading at the leading edge making a bubble-burst more likely. Also in Gault's experiment the ratio of the chord of the model to the height of the tunnel is

rather large ($(c/h) = \frac{1}{2}$) and the constraint of the flow by the tunnel walls induces an effective camber in the flow in comparison to the results in free air. The lift coefficient in free air can be obtained by subtracting a correction term which is approximately equal to $(\pi^2/24)(c/h)^2(C_L + 2C_m)$ and takes the value 0.109 at an incidence of 9 degrees. The effective camber in the flow is illustrated in Fig 10 where the viscous lift from Gault's experiment appears to be larger than the inviscid lift at any particular incidence. The induced camber in the flow is also illustrated in Fig 11 where the inviscid and viscous pressure distributions around the nose are compared at lift coefficients of 1.02: in contrast to the expected behaviour, the suction peak for the inviscid pressure distribution is larger than the peak for the viscous pressure distribution. Wood² did not include either of these effects, which explains his failure to reproduce the experimental behaviour of the bubble. However, if the experimental pressure distributions are used, then the experimental growth of the bubble is adequately predicted by Horton's method.

In Fig 11 the predicted points of laminar separation and turbulent reattachment are indicated for inviscid and experimental pressure distributions at a lift coefficient of 1.02. The difference is quite marked: the calculation for the experimental pressure distribution is in reasonable agreement with the perturbation caused by the bubble; for the inviscid pressure distribution the prediction of separation is premature.

For this experiment it is difficult to take account of the camber induced by the tunnel constraint, which masks the usual viscous effects, and to predict the experimental pressure distribution. As it is not possible to calculate the pressure distribution for which the bubble is about to burst, this is a poor test case for the prediction of bubble bursting. A better test case is provided by Woodward's experiment³ on a 12.2% RAE 100 section which is discussed in the next section.

4.2 12.2% thick RAE 100 aerofoil section

The change in character of the stall on the 12.2% thick RAE 100 section with increasing Reynolds number gives a good test case for the prediction of bubble bursting. Woodward³ reported that at Reynolds numbers less than 0.60×10^6 the section exhibited a leading-edge stall arising from a bubble-burst; whilst at Reynolds numbers greater than 0.60×10^6 the section has a trailing-edge stall (see Fig 16). The prediction of the low Reynolds number stalling behaviour by Horton's method is examined for the experimental and inviscid pressure distributions. This method is also checked against the observed change in stalling behaviour with increased Reynolds number.

The lift curve for a Reynolds number of 0.55×10^6 shown in Fig 12 exhibits the rapid decrease in lift at the stall which characterises a leading-edge stall. The inviscid lift curve is also shown in Fig 12 and, in contrast to Fig 10, for this two-dimensional experiment the inviscid lift is larger than the experimental lift at comparable incidences. In the calculation of the bubble for the inviscid pressure distributions two values of the constant defining the length of the laminar bubble have been used: for $c = 4$ the angle of incidence at which the bubble bursts is well-predicted but the corresponding lift coefficient is too large; whereas for $c = 5$ the incidence for the predicted bubble-burst is too low but the lift coefficient is in better agreement.

In Fig 13 the comparison of the inviscid and experimental pressure distributions at a lift coefficient of 1.069 (corresponding to an experimental incidence of 13°) shows the increased forward-loading induced by the viscous effects. This difference again leads to a marked difference in the prediction of laminar separation. The perturbation caused by the bubble has been removed from the experimental pressure distribution; the straightforward boundary-layer calculation should then give a more faithful representation of the flow close to separation. Close to separation the pressure becomes a dependent variable and the calculation method should then change from a parabolic to an elliptic type. However for a simple design procedure the parabolic method is considered to be adequate as long as the experimental pressure distribution is modified. The positions of reattachment for two lengths of laminar bubble are shown in Fig 13 and for $c = 4$ the prediction for the experimental case agrees well with the observed bubble. In Fig 14 the loci of points of reattachment are given for the inviscid pressure distribution at a lift coefficient of 1.069 and these should be compared with the loci for the modified experimental pressure distributions in Fig 15. This lift coefficient is just below the maximum value and the calculation with $c = 5$ for the experimental pressure distribution indicates correctly that the bubble is about to burst.

Although the calculations for the inviscid pressure distribution are not so precise it was shown in Fig 12 that with $c = 5$ bubble bursting is predicted at a slightly higher lift coefficient of 1.19. The inviscid pressure distribution gives reasonable guidance on the prediction of bubble bursting of calculations are performed at values of lift corresponding to those from experiment rather than at the comparable incidence.

The change in the nature of the stall with increasing Reynolds number is indicated on Fig 16 and the ability of Horton's method to predict this behaviour

is indicated on Fig 17. An inviscid pressure distribution with a lift coefficient of 1.305 has been selected as this is representative of pressure distributions which would have occurred if the flow had not separated. For a Reynolds number of 0.55×10^6 the bubble bursts, whilst at higher Reynolds numbers the bubble remains attached. For a Reynolds number of 0.91×10^6 a trailing-edge separation would have already provoked a stall. Fig 16 indicates that at the highest Reynolds number the stall is at 14° incidence and caused by a trailing-edge separation and in Fig 18 Horton's method used for the modified experimental pressure distribution predicts a reattaching bubble. However the location of the bubble does not quite agree with the experimental observations. This is caused by the poor definition of the pressure distribution arising from the small number of experimental points and the difficulty in estimating the shape of the pressure distribution with the bubble removed.

Although Horton's method gives reasonable agreement with the experimental results it is unsatisfactory that the modified experimental pressure distributions are used and the bursting prediction cannot be checked precisely. These problems could be overcome by calculating the viscous flow around the aerofoil at the appropriate incidences. However this approach is thwarted by the presence of separated flow at the trailing edge for angles of incidence below the stall. An inverse method⁸ has been given for calculating the development of a separated boundary layer but it has not yet been incorporated into a full viscous calculation.

In conclusion Horton's method gives a reasonable prediction of bubble growth and bursting when the modified experimental pressure distribution is used. An inviscid pressure distribution which has been matched to the experimental lift coefficient gives a less accurate description of the bubble but this approach could still be useful for a design procedure.

5 ALTERNATIVE PREDICTION METHODS

In the following section the separated shear layer is assumed to be an equilibrium flow after transition and using some results from East, *et al.*⁸ a simple algebraic expression for the pressure recovery is derived: the complicated integration in Horton's method is replaced by the simple algebraic expression.

If it is assumed that the separated turbulent shear layer develops with zero skin friction and if it is further assumed that this layer is an equilibrium flow, then a pressure recovery may be predicted. In such an equilibrium flow the momentum will grow linearly (East, *et al.*⁸) and approximately

$$\theta \approx \theta_c + 0.02(x - x_c) , \quad (2)$$

where c refers to conditions at the start of the pressure rise. For equilibrium flows, East, *et al.*⁵ also showed that

$$\frac{\theta}{u_e} \frac{du_e}{dx} \approx -0.004 ; \quad (3)$$

thus

$$\frac{\theta}{u_e} \frac{du_e}{d\theta} \approx -0.2 , \quad (4)$$

which can be integrated to give

$$\left(\frac{u_e}{u_{e_s}}\right)^2 = \left(\frac{\theta_s}{\theta}\right)^{0.4} . \quad (5)$$

The pressure rise can then be calculated from Bernoulli's equation in the form

$$C_p = 1 - \left(\frac{u_{e_s}}{u_\infty}\right)^2 \left(\frac{\theta_s}{\theta}\right)^{0.4} . \quad (6)$$

The start of the pressure rise is taken to be the end of the laminar portion of the bubble which is calculated by the correlation of Horton with $c = 5$. The momentum thickness of the boundary layer has been calculated upto separation and by examination of the momentum integral equation we conclude that this value should be used at the start of the pressure rise. The momentum integral equation for a laminar boundary layer is

$$\delta_1 u_e \frac{du_e}{dx} = \frac{\tau_w}{\rho} - \frac{d}{dx} \left(u_e^2 \theta\right) . \quad (7)$$

For the separated boundary layer we have

$$\tau_w = 0 , \quad (8)$$

and

$$\frac{du_e}{dx} = 0 , \quad (9)$$

thus

$$\frac{d}{dx} \left(u_e^2 \theta\right) = 0 ,$$

which implies that the momentum thickness is constant.

In Fig 19 the pressure rise determined by the assumption of an equilibrium flow is compared with the locus of possible reattachment points for the modified viscous pressure distribution on RAE 100 at a lift coefficient of 1.069 (cf Fig 15). The point of intersection of the pressure rise with the pressure distribution is interpreted as the first possible position for reattachment. At this point the value of the Crabtree parameter σ is 0.36 which being larger than 0.35 indicates that the bubble has burst. In Fig 15 we saw that Horton's method predicted that the bubble was on the point of bursting. It is unlikely that the separated shear layer is an equilibrium flow immediately after transition or before reattachment: Horton found the value of $(\theta/u_e)(du_e/dx)$ at reattachment to be -0.0082 compared to the value of -0.004 for an equilibrium layer. The departure of the separated shear layer from equilibrium would account for the discrepancy between the two predictions of bubble bursting. However the simple method still provides a useful guide to the behaviour of the bubble. For example in Fig 20 the effect of increasing Reynolds number is examined by repeating the calculations of Fig 17 for the inviscid pressure distribution for RAE 100 with a lift coefficient of 1.305. For the Reynolds numbers 0.55×10^6 , 0.91×10^6 and 1.78×10^6 , the values of the parameter σ are 0.368, 0.25 and 0.126 respectively; the bubble-bursts at the lowest Reynolds number but remains attached at the other Reynolds numbers which agrees with the prediction by Horton's method. It is concluded that the separated turbulent shear layer is almost an equilibrium flow so that a simple test for bubble bursting can be developed.

6 CONCLUSIONS

Horton's method gives a useful description of the growth and bursting of laminar bubbles. An examination of the usual parameters for predicting bubble-bursting can be misleading and it is recommended that a graphical examination of the relationship between the locus of possible reattachment positions and the pressure distribution will give a clearer prediction of the burst. The pressure distributions must be defined by sufficient points to ensure that the position of laminar separation is predicted accurately. If the pressure distribution is defined by a few points and only the simple bubble parameters are examined, then it has been shown that incorrect conclusions will be drawn about the bursting of the bubble.

The assumption that the separated turbulent shear layer is an equilibrium flow leads to a simple method of detecting a bubble-burst. This method does not provide sufficient information for the completion of the calculation of the

development of the boundary layer after reattachment and Horton's method must be used for the calculation of a full viscous solution.

The semi-empirical method of Horton provides an adequate description of the growth and bursting of laminar separation bubbles on two aerofoils at various Reynolds numbers and the slat of a high-lift wing. It can be used with increased confidence in the design of high-lift wings for wind-tunnel models.

Table 1
COMPARISON OF PARAMETERS FOR LAMINAR BUBBLE

Condition	Tapered model			Panel model	End-plate model
	α_1	α_2	α_3		
Reynolds number based on slat chord normal to leading edge	184000	184000	184000	190000	439000
θ separation	0.00030	0.00035	0.00029	0.00030	0.00018
$(R\delta_1)$ separation	999	1143	995	1003	1406
$(R\theta)$ separation	270	309	269	271	380
σ	0.14	0.34	0.14	0.16	0.08

Table 2
EFFECT OF REDUCING NUMBER OF POINTS IN PRESSURE DISTRIBUTION

Condition	$\left(\frac{s}{c}\right)$ separation	σ	$R_{\theta s}$	Length of bubble
Tapered model α_2	0.445	0.34	309	0.074
Tapered model reduced number of points α_2	0.411	0.15	270	0.059

LIST OF SYMBOLS

c	constant in expression for length of laminar bubble
C _p	pressure coefficient
h	height of tunnel
ℓ ₁	length of laminar bubble = $(c \times 10^4)/(Reu_s)$
m	pressure gradient parameter = $(\theta^2/\nu)(dU/dx)$
Re	Reynolds number
R _{δ₁}	Reynolds number based on displacement thickness
R _θ	Reynolds number based on momentum thickness
u	velocity
α	angle of incidence
δ ₁	displacement thickness of boundary layer
Λ	pressure gradient parameter = $(\theta/u_e)(du_e/dx)$
θ	momentum thickness of boundary layer
ρ	density
σ	pressure recovery factor = $(Cp_r - Cp_s)/(1 - Cp_s)$
τ _w	shear stress at the wall
ν	kinematic viscosity

Suffices

e	denotes conditions at the edge of the viscous layer
c	condition at start of pressure rise
r	condition at point of reattachment
s	condition at point of separation

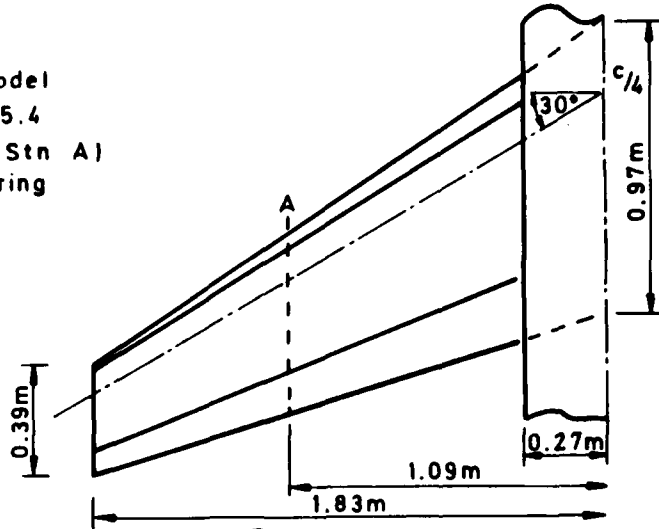
REFERENCES

<u>No.</u>	<u>Author</u>	<u>Title, etc</u>
1	H.P. Horton	A semi-empirical theory for the growth and bursting of laminar separation bubbles. ARC CP 1073 (1967)
2	I.W. Wood	A test of Horton's theory for the bursting of laminar separation bubbles using two NACA aerofoils. HSA Brough, Note YAD 3162
3	D.S. Woodward	The two-dimensional characteristics of a 12.2% thick RAE 100 aerofoil section. ARC R&M 3648 (1971)
4	P.R. Owen L. Klanfer	On the laminar boundary-layer separation from the leading edge of a thin aerofoil. ARC CP 220 (1953)
5	L.F. Crabtree	The formation of regions of separated flow on wing surfaces. ARC R&M 3122 (1959)
6	B. Thwaites (Ed)	Incompressible aerodynamics. Clarendon Press (1960)
7	D.E. Gault	Boundary-layer and stalling characteristics of the NACA 63-009 airfoil section. NACA TN 1894
8	L.F. East P.D. Smith P.D. Merryman	Prediction of the development of separated turbulent boundary layers by the lag-entrainment method. RAE Technical Report 77046 (1977)

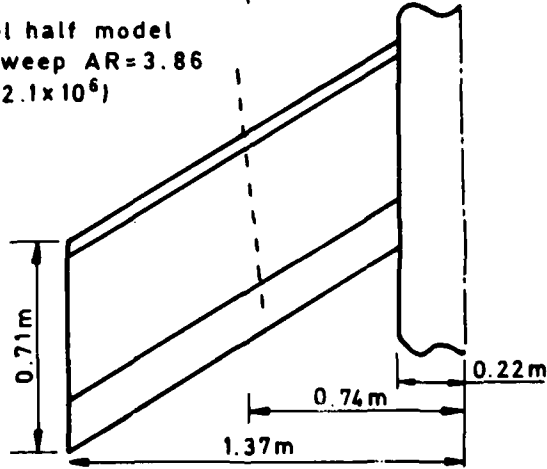
REPORTS CITED ARE NOT NECESSARILY
AVAILABLE TO MEMBERS OF THE PUBLIC
OR TO COMMERCIAL ORGANISATIONS

Fig 1

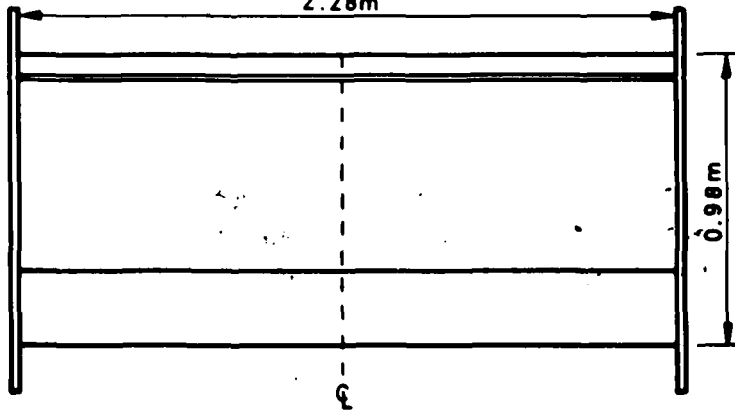
(1) Tapered half model
30° sweep AR=5.4
(Re=2.2x10⁶ at Stn A)
Pressure measuring
station - - - -



(2) Panel half model
31° sweep AR=3.86
(Re=2.1x10⁶)



(3) End plate model AR=2.31 (Re=3.6x10⁶)



TR 80060

Fig 1 Planforms of wind-tunnel models

Fig 2

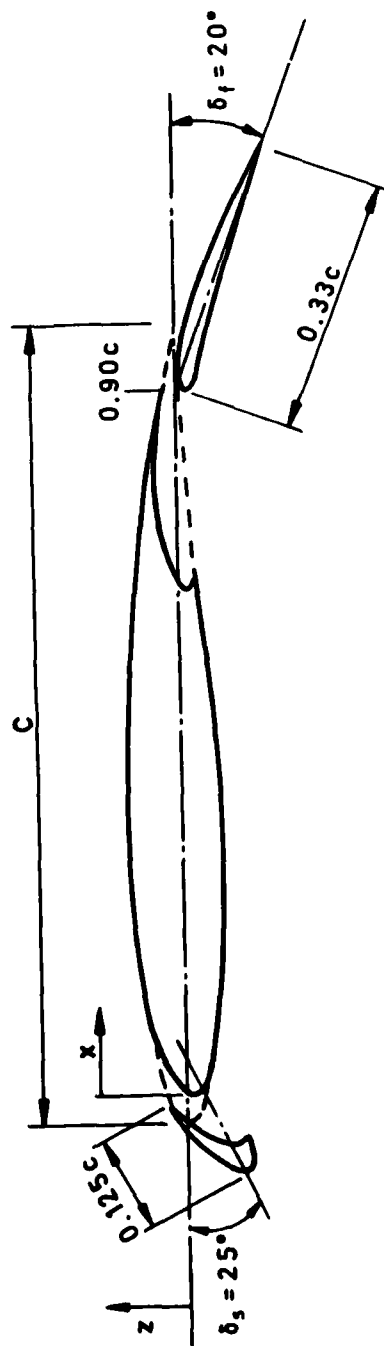


Fig 2 Aerofoil configuration for comparative tests

Fig 3

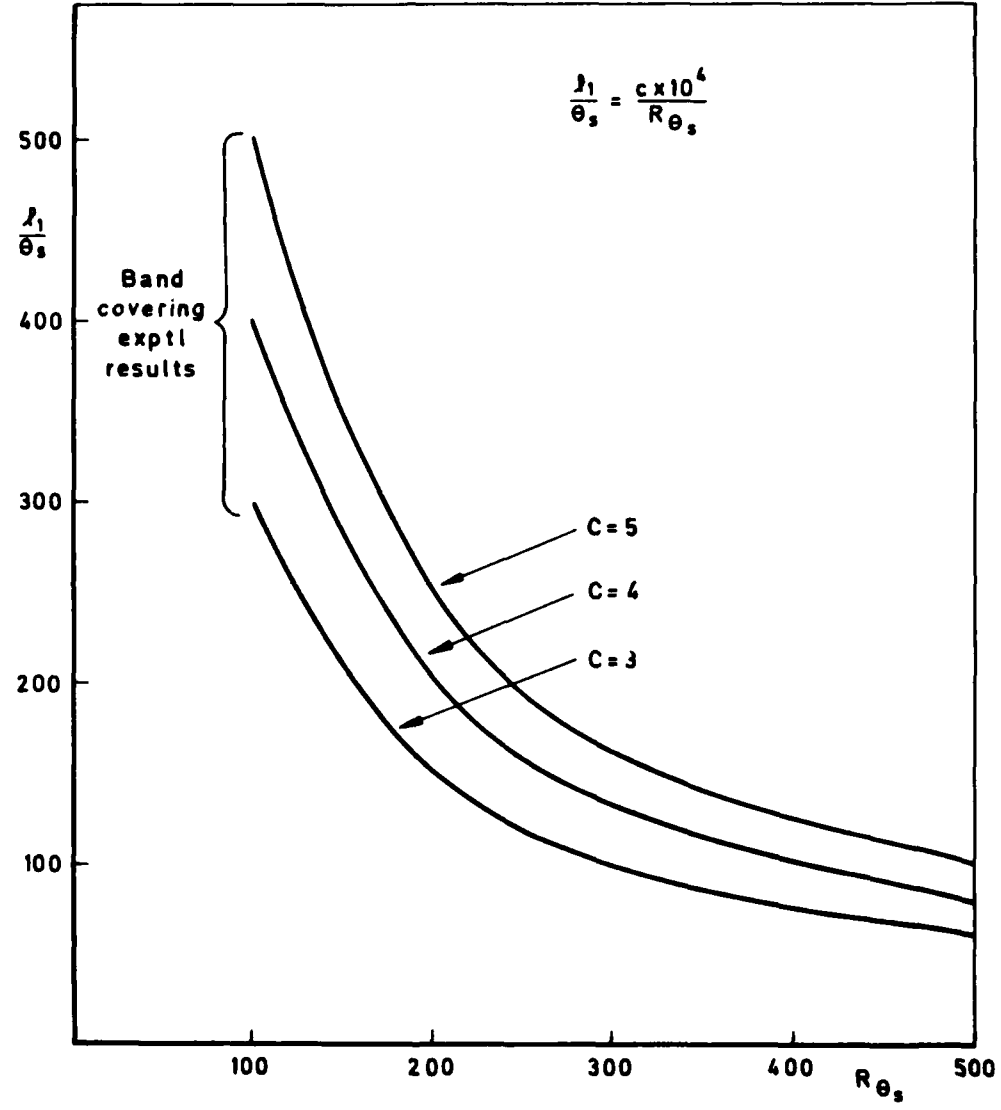


Fig 3 Length of laminar bubble

TN 90090

Fig 4

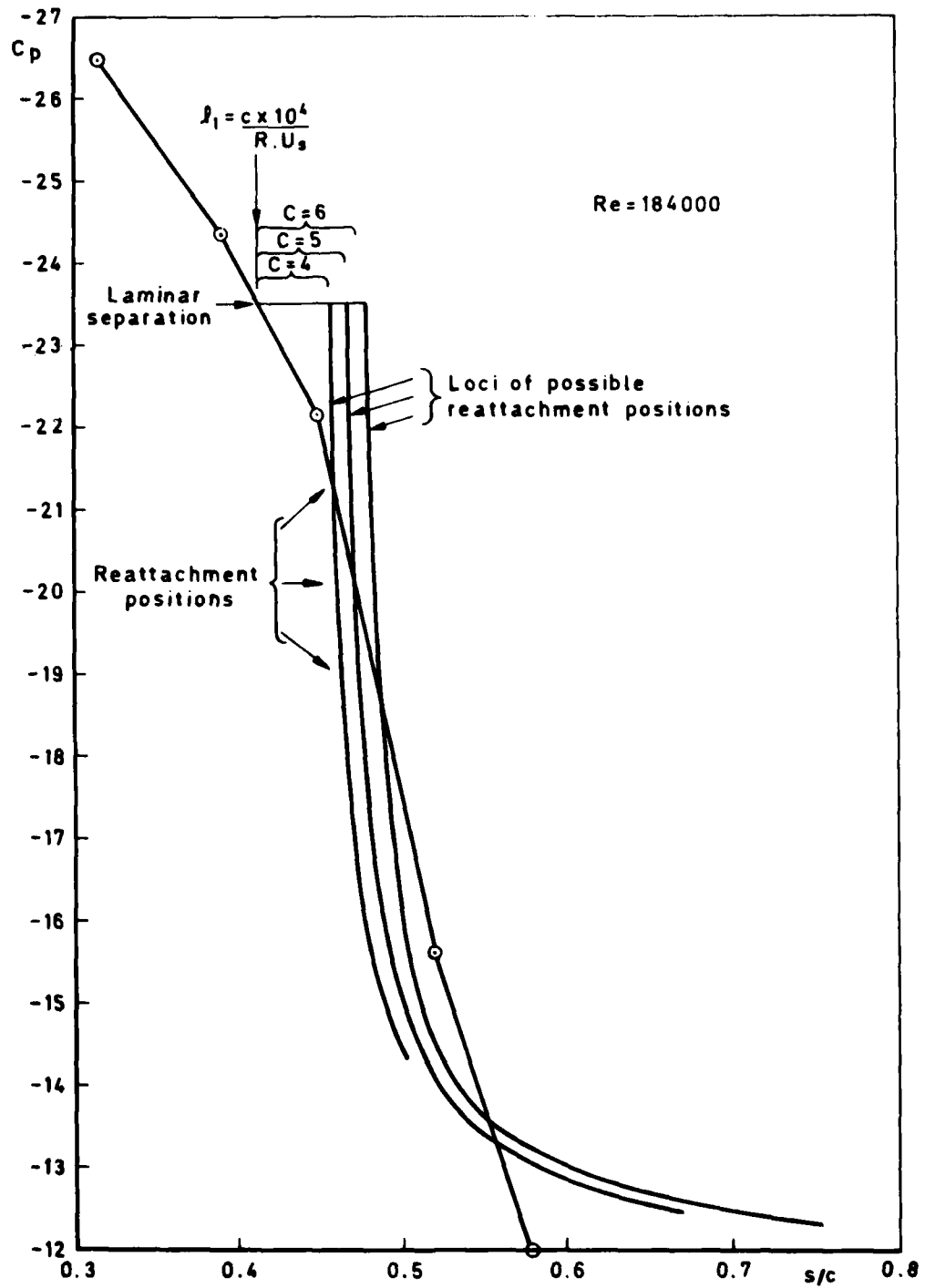


Fig 4 Slat pressure distribution at α_1 for slat of tapered model

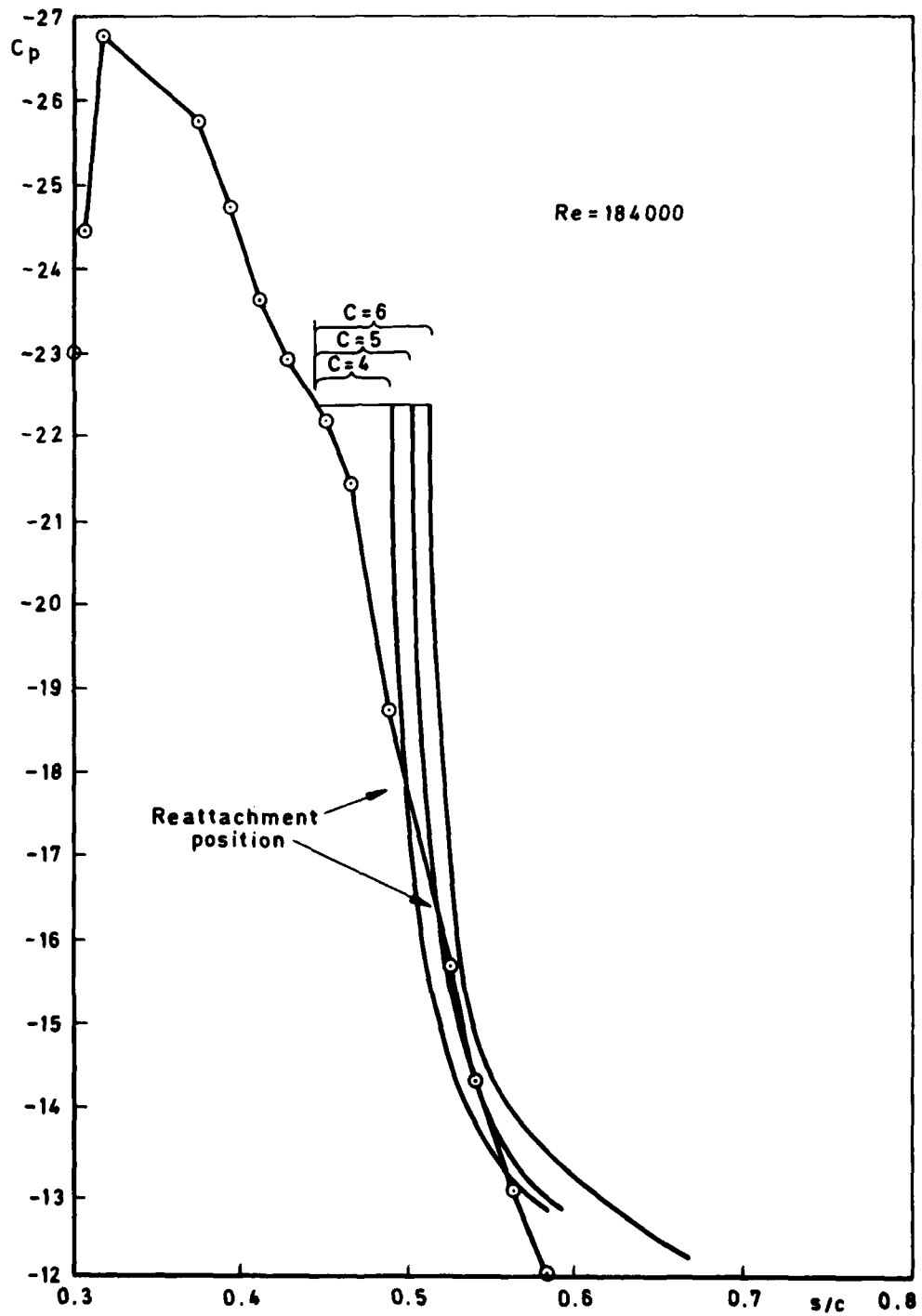


Fig 5 Slat pressure distribution at α_2 for slat of tapered model

Fig 6

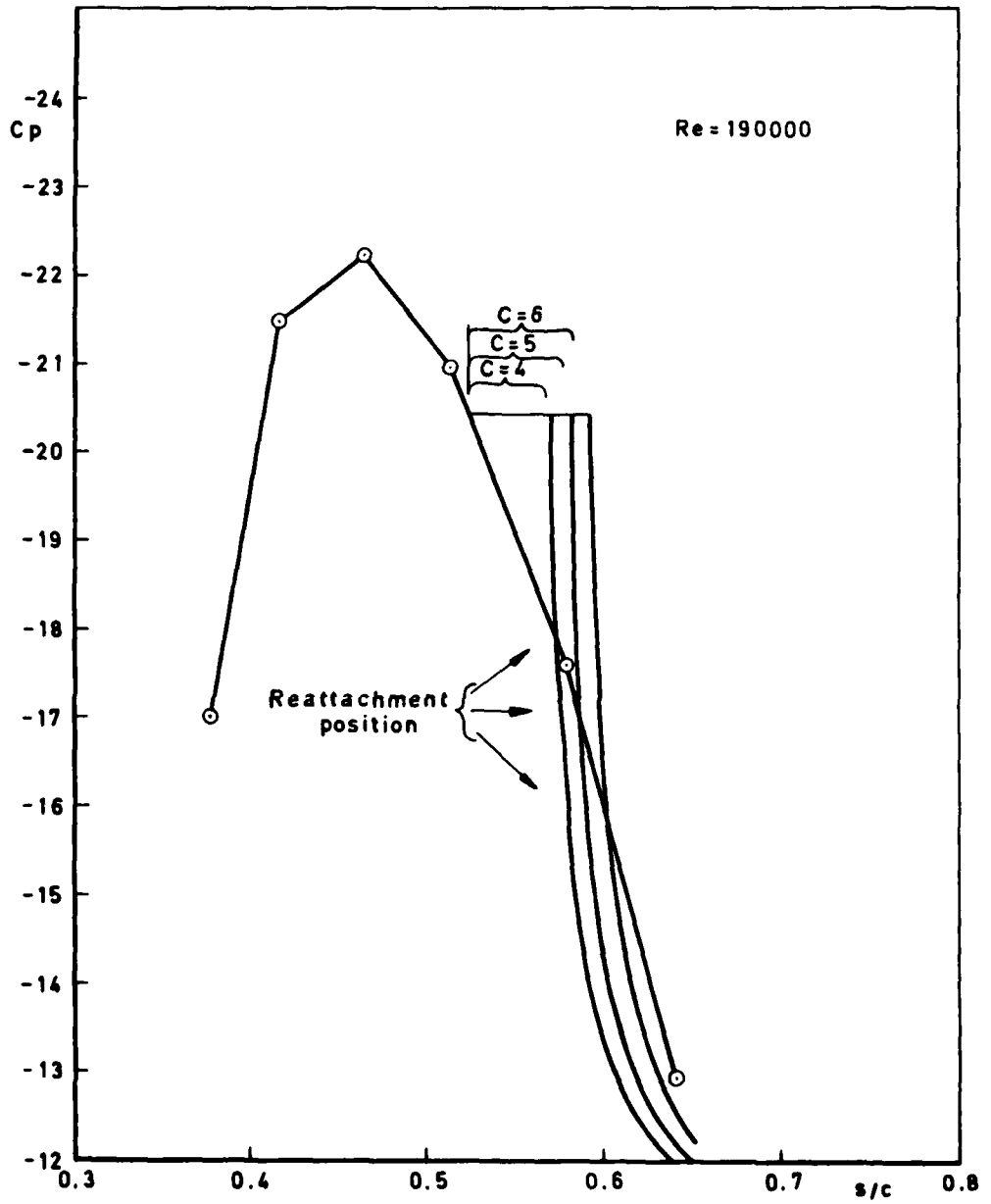
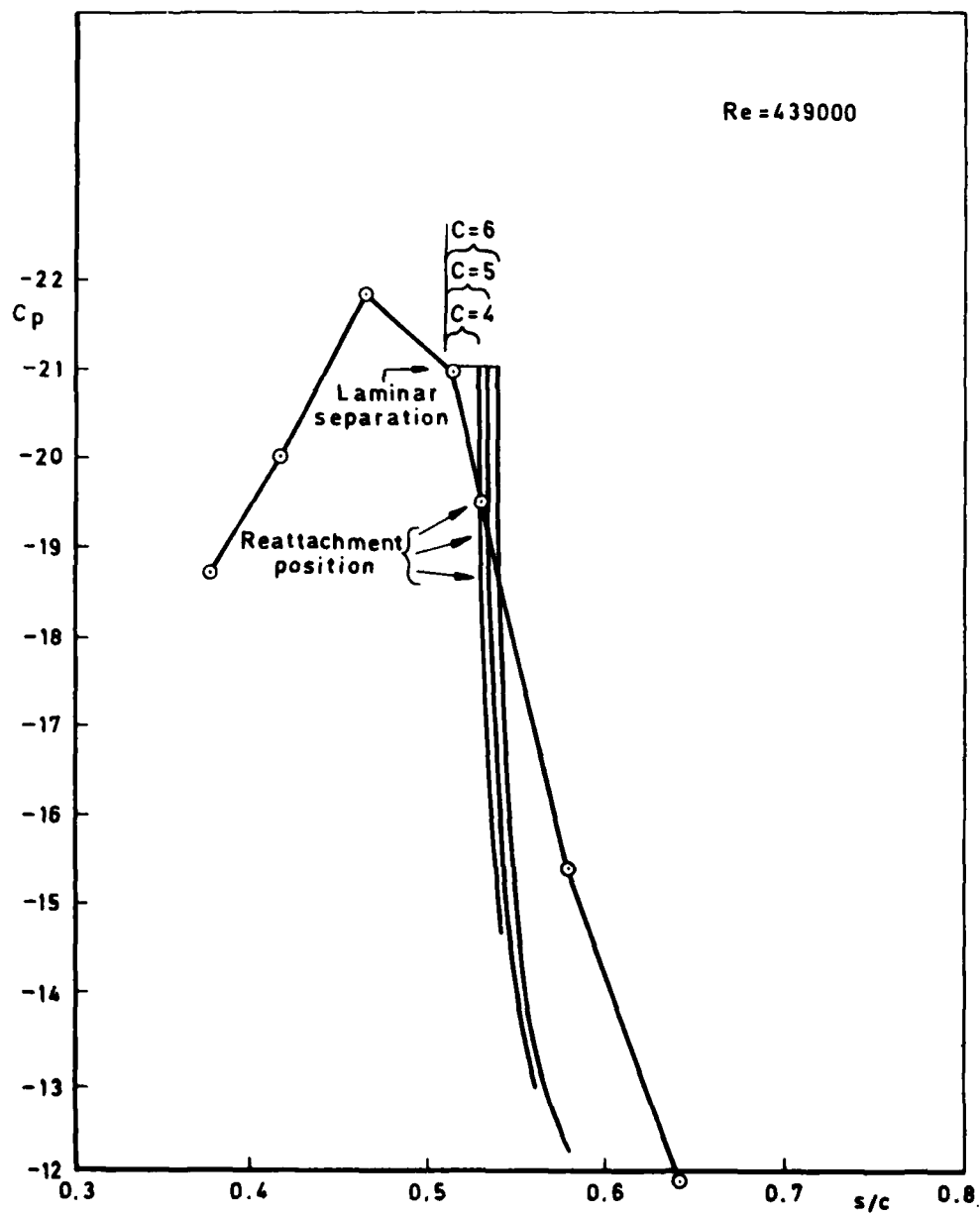


Fig 6 Pressure distribution for the slat of the swept panel model

Fig 7



TR 80060

Fig 7 Pressure distribution for the slit of the end-plate model

Fig 8

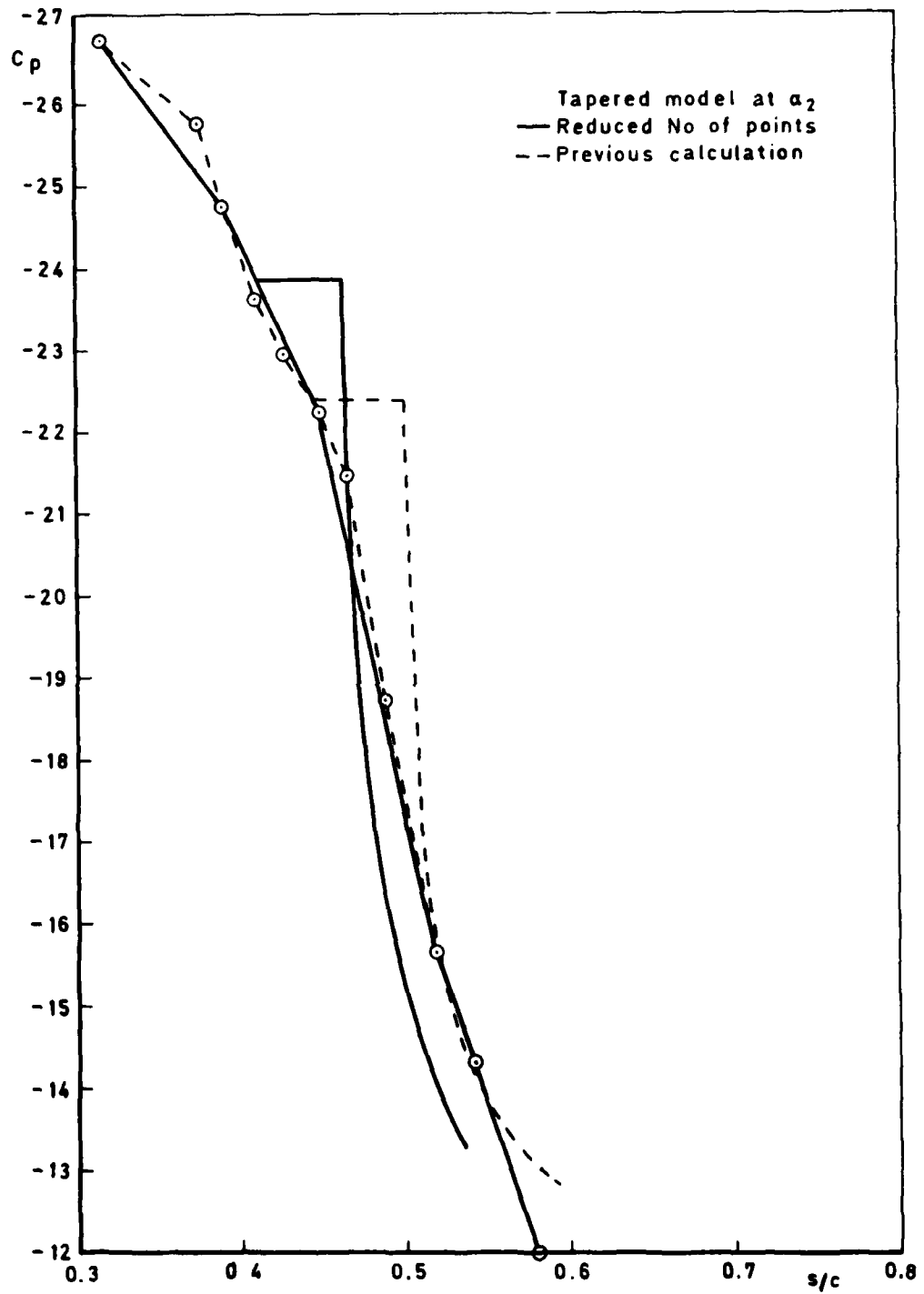
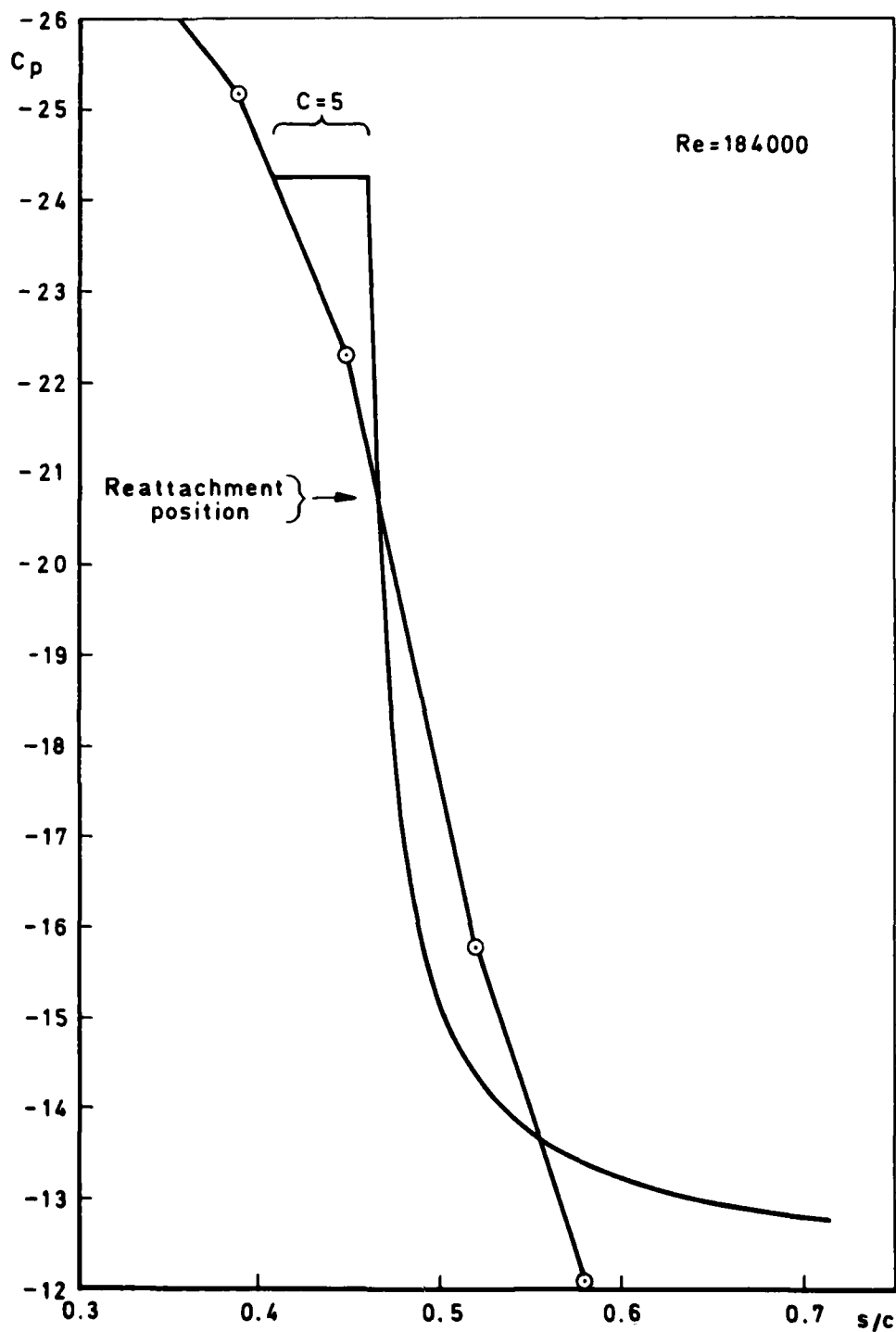


Fig 8 Effect of reducing number of points defining pressure distribution



TR 80060

Fig 9 Slat pressure at α_3 (derived) for the slat of the tapered model

Fig 10

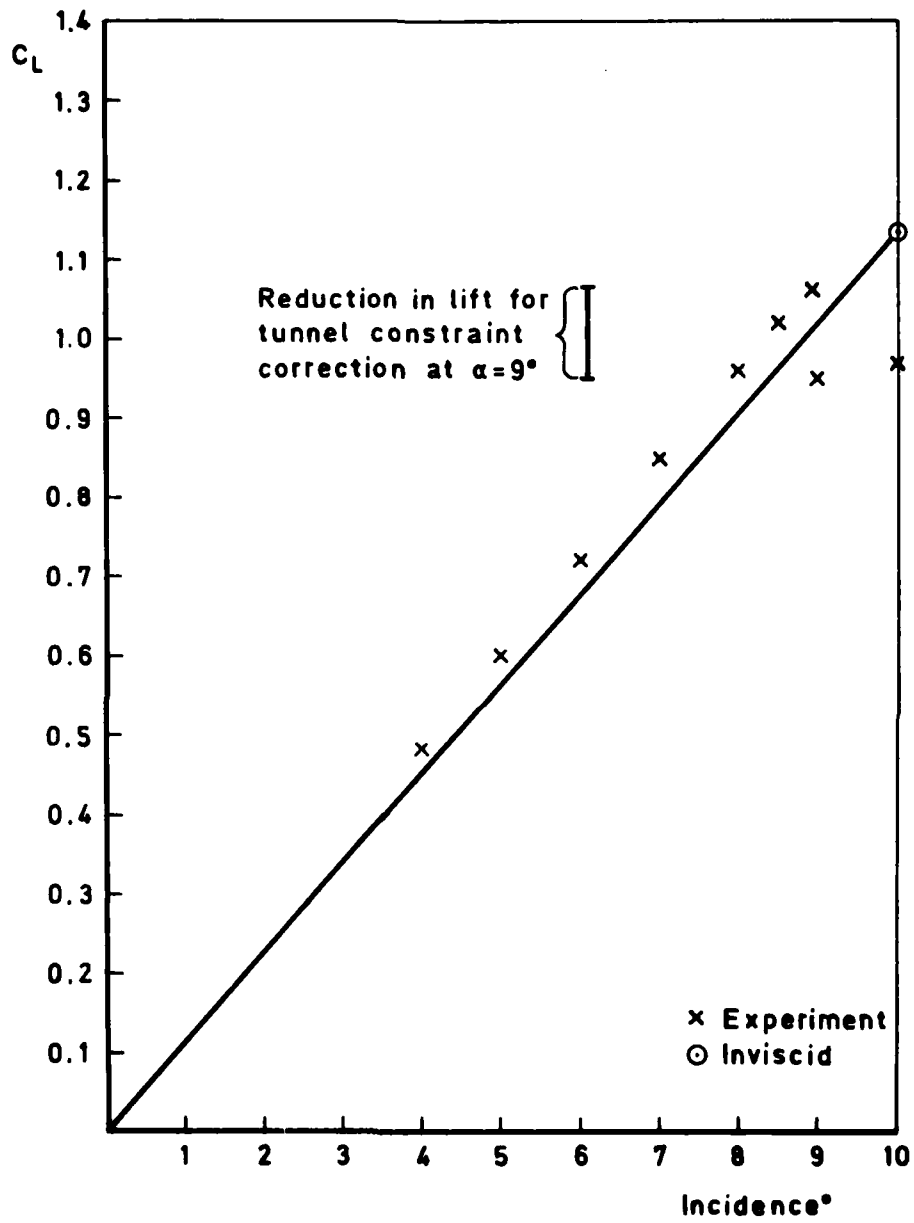


Fig 10 Comparison of experimental and inviscid lift curves for NACA 63-009

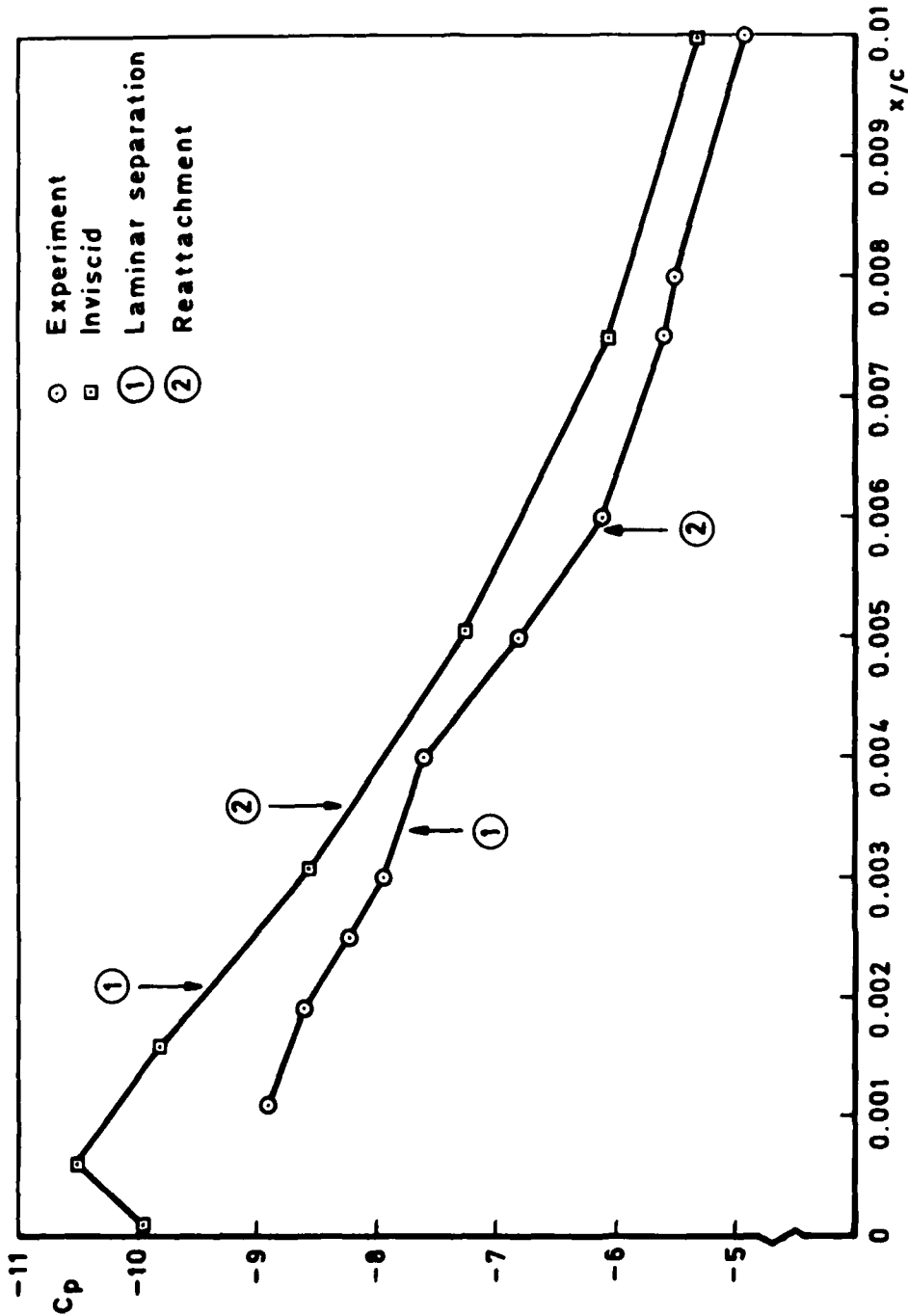


Fig 11 Comparison of bubble predictions on inviscid and experimental pressure distributions for NACA 63-009, $C_L = 1.02$

Fig 12

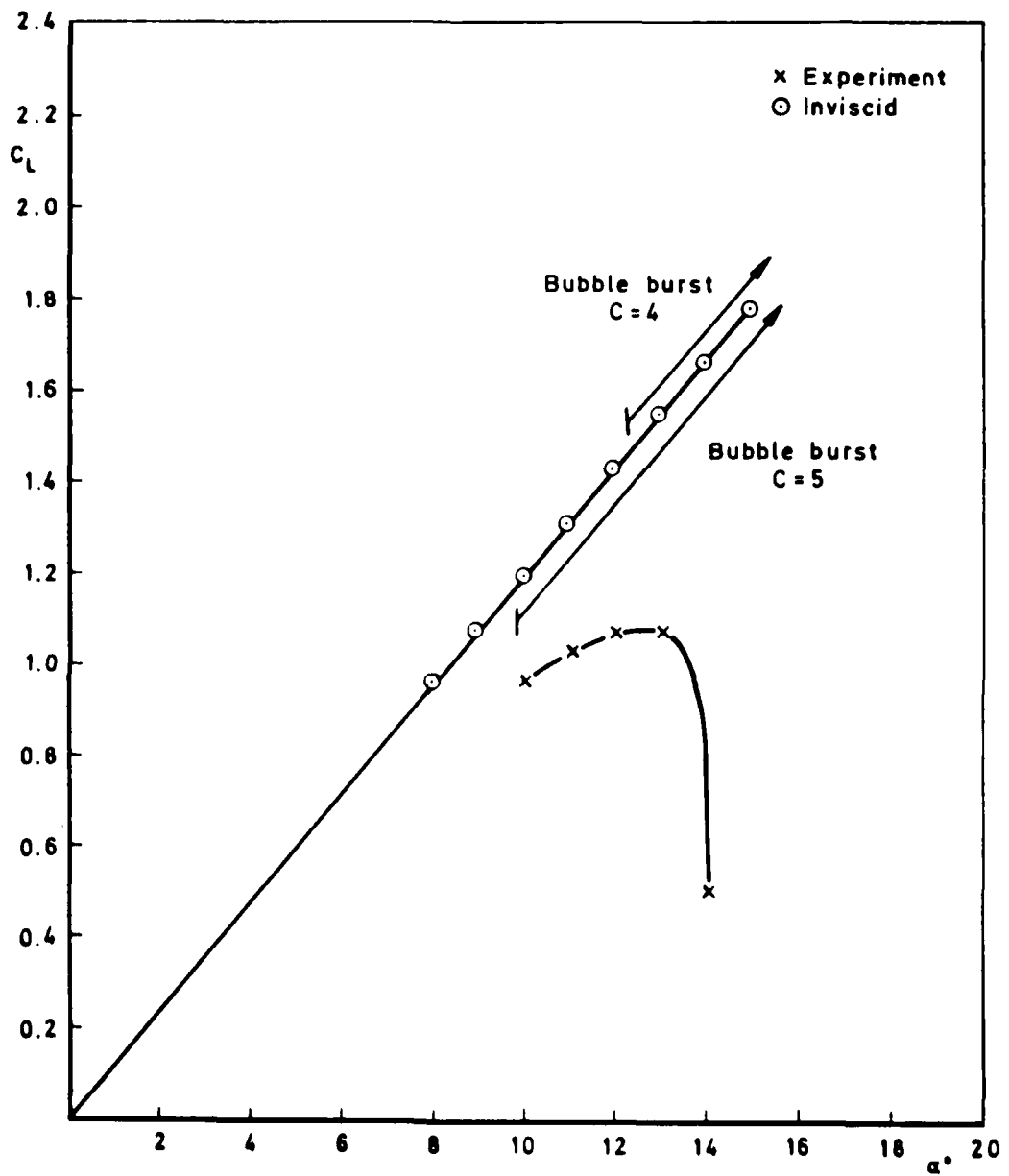


Fig 12 RAE 100 lift variation with incidence. $Re = 0.55 \times 10^6$

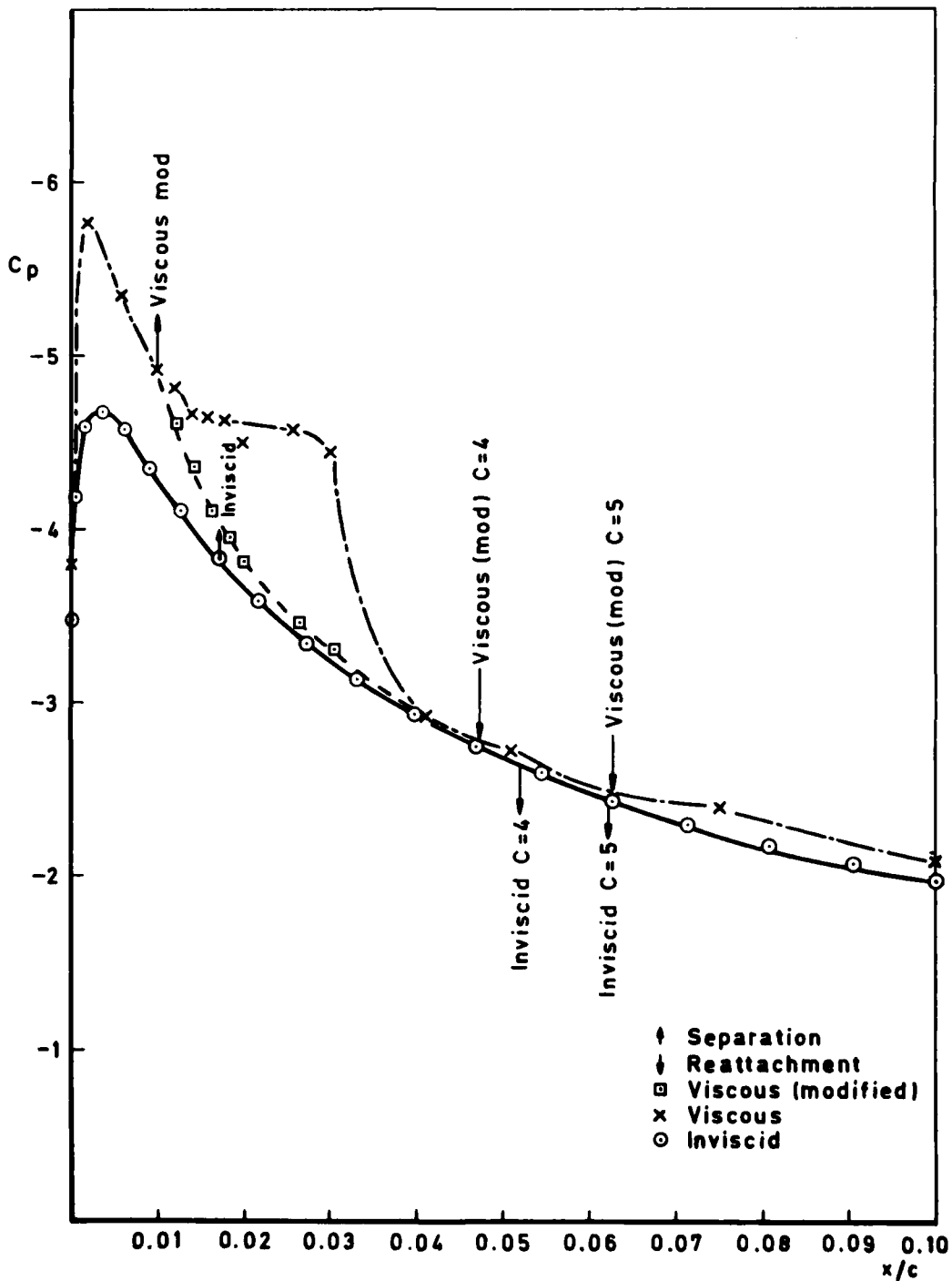


Fig 13 Comparison of viscous and inviscid pressure distributions. $Re = 0.55 \times 10^6$, $C_L = 1.069$

Fig 14

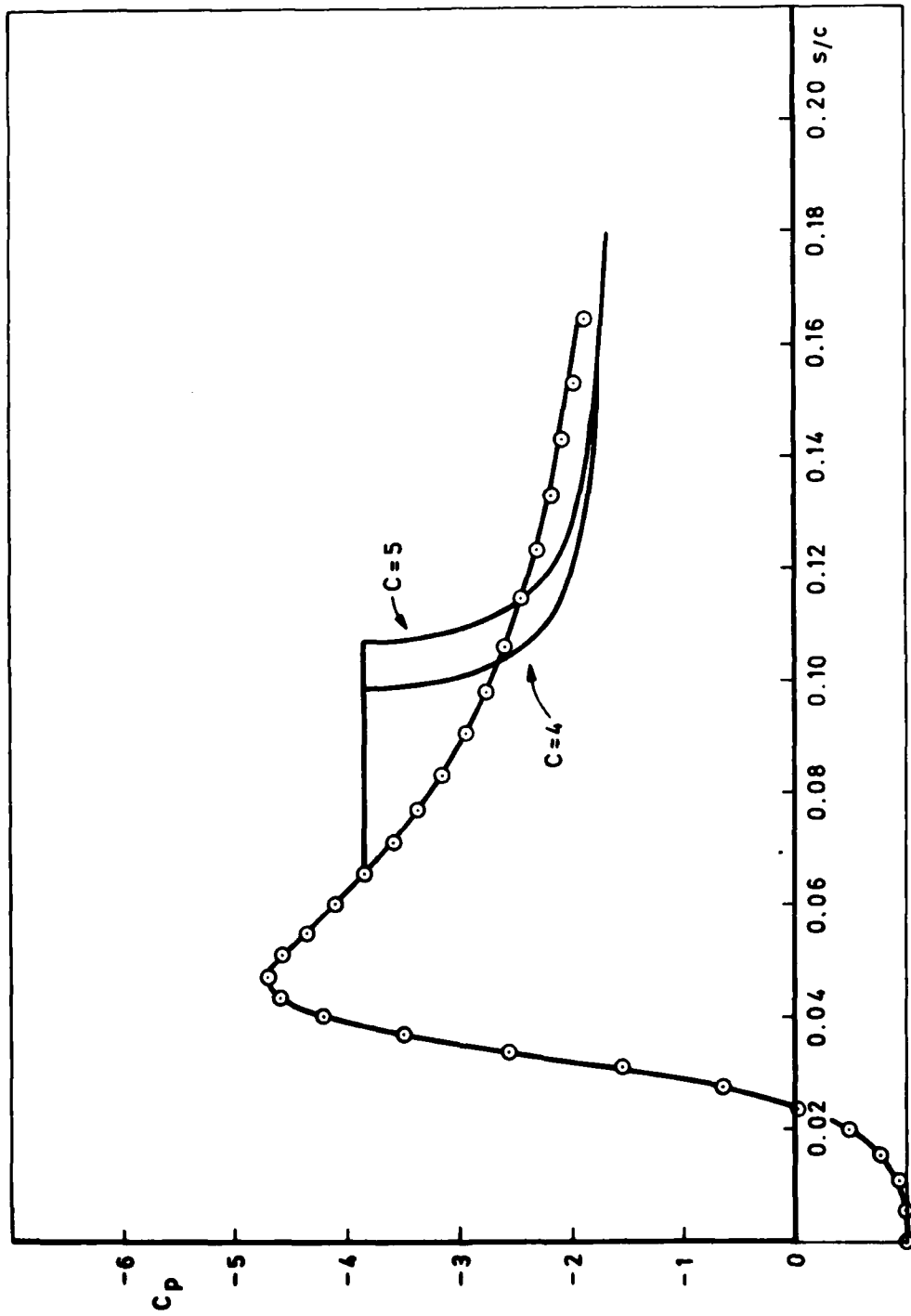


Fig 14 Locus of reattachment positions on inviscid pressure distribution for RAE 100 at $C_L = 1.069$

TR 80060

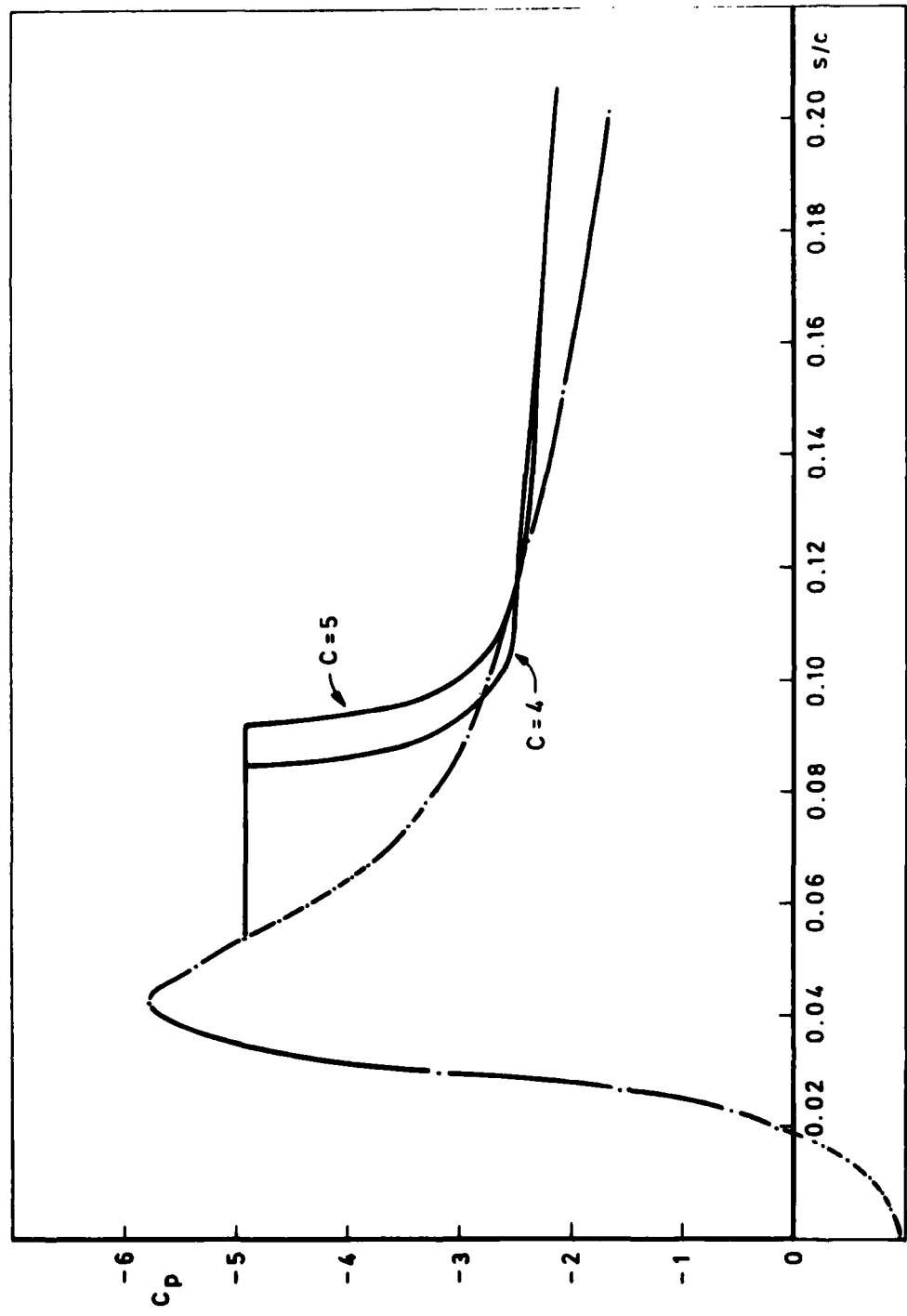


Fig 15 Locus of reattachment positions on the viscous pressure distribution for RAE 100 at $C_L = 1.069$, $Re = 0.55 \times 10^6$

Fig 16

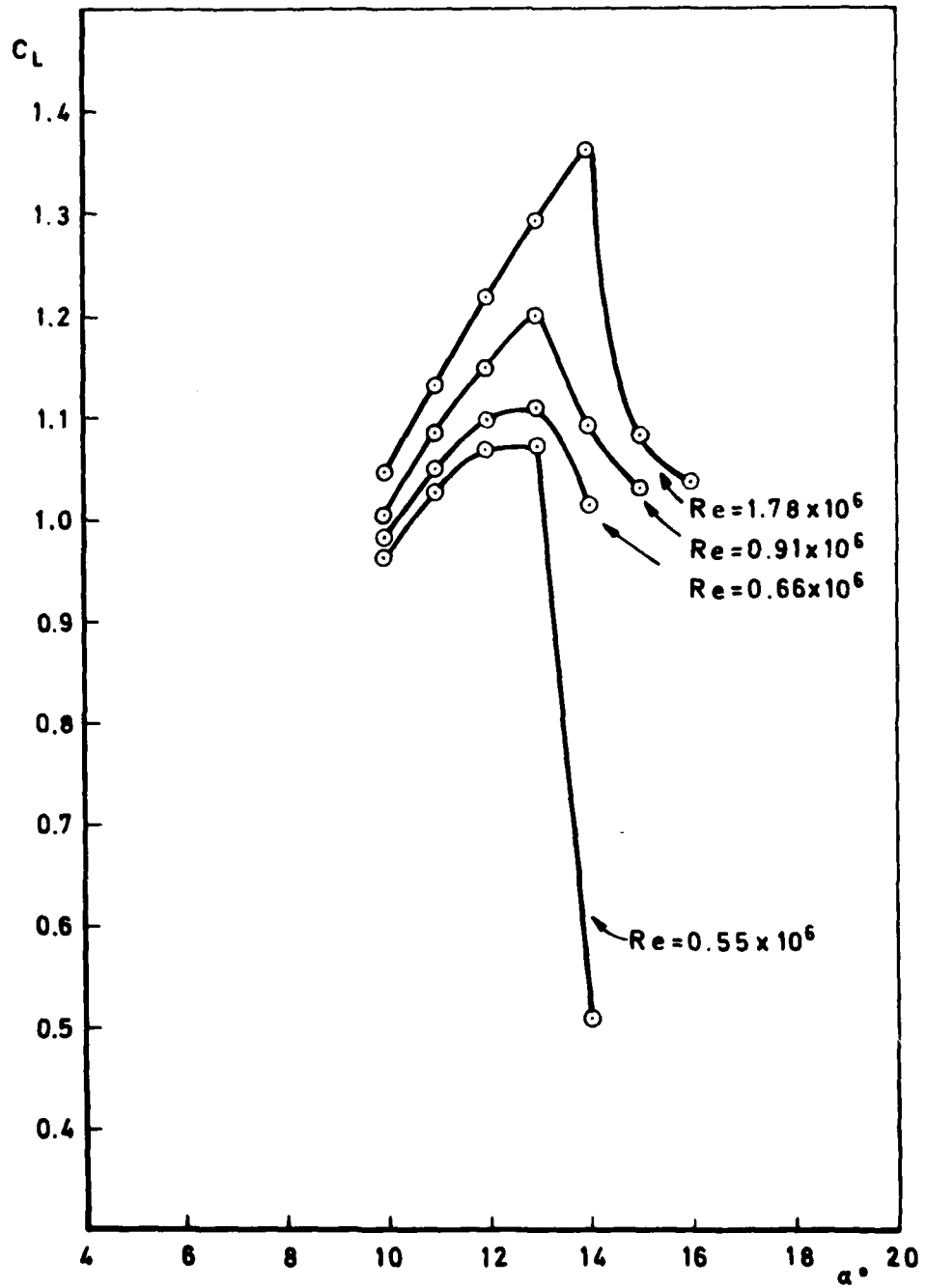


Fig 16 Variation of experimental lift with Reynolds number: RAE 100 section

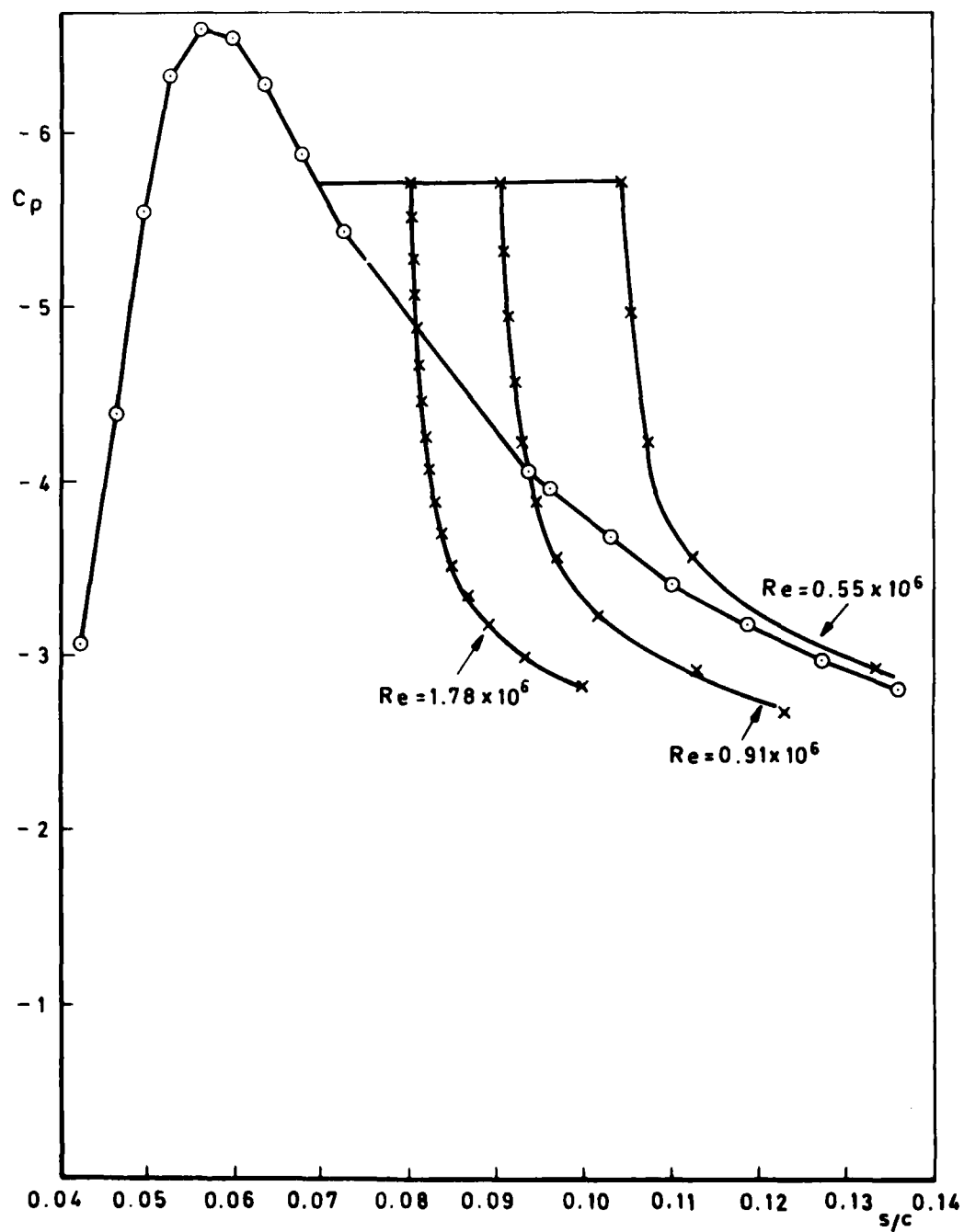


Fig 17 RAE 100 inviscid pressure distribution, variation of Re , $\alpha = 10.87$, $C_L = 1.305$, $c = 5$

Fig 18

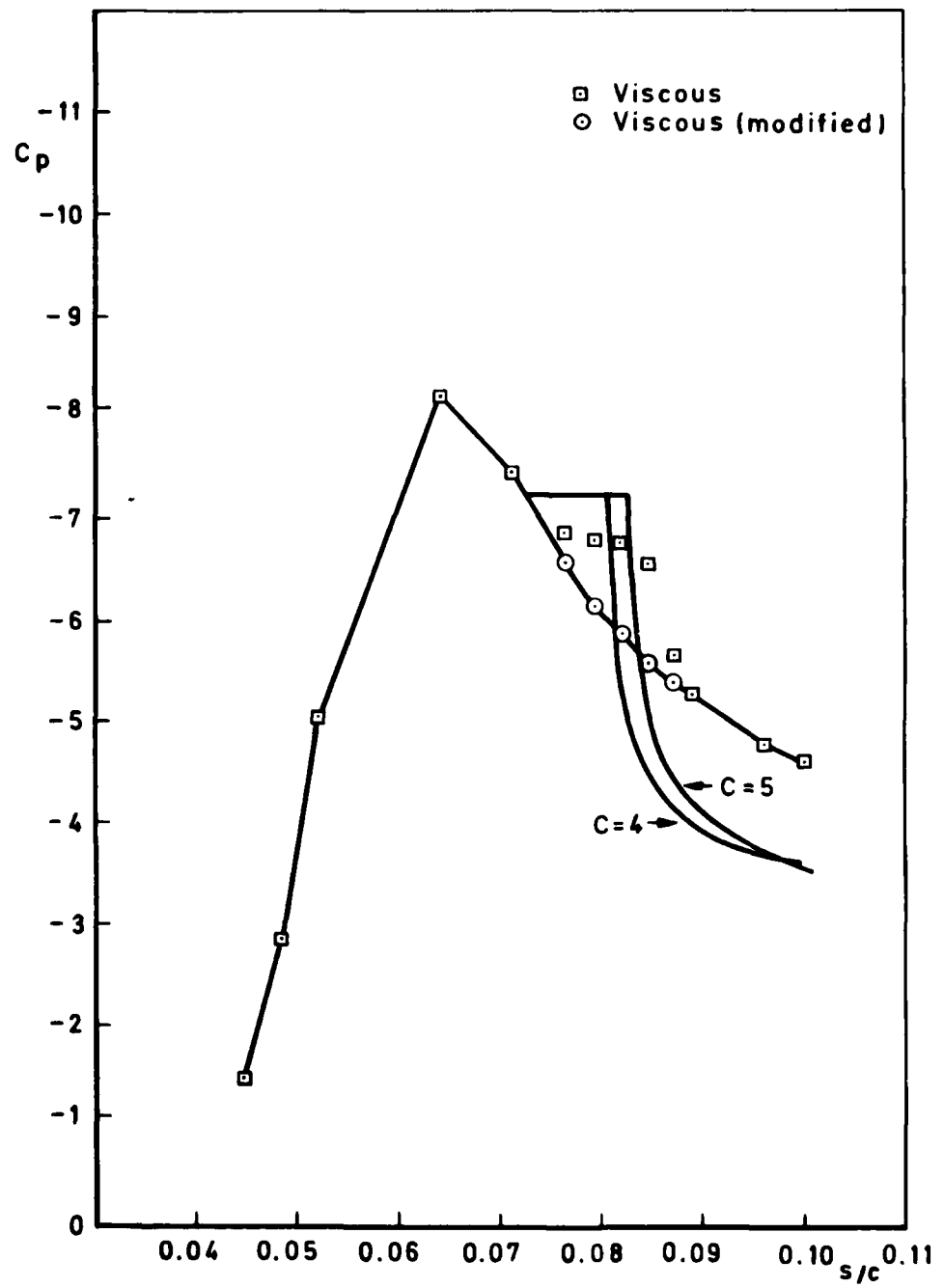


Fig 18 RAE 100 viscous pressure distribution, $\alpha = 14^\circ$, $Re = 1.78 \times 10^6$

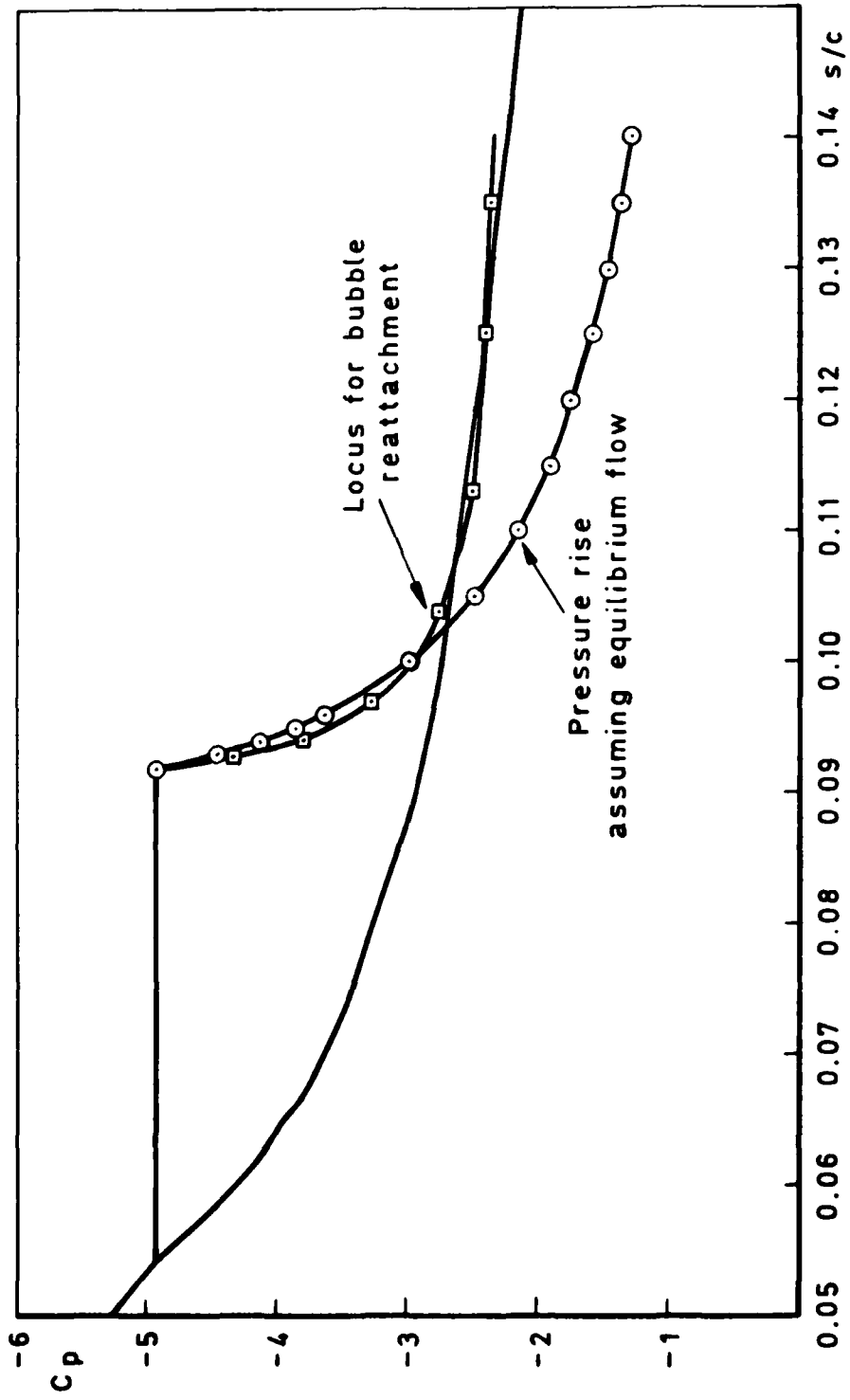


Fig 19 Prediction of bubble bursting by assuming equilibrium flow: RAE 100, $C_L = 1.069$, $Re = 0.55 \times 10^6$

Fig 20

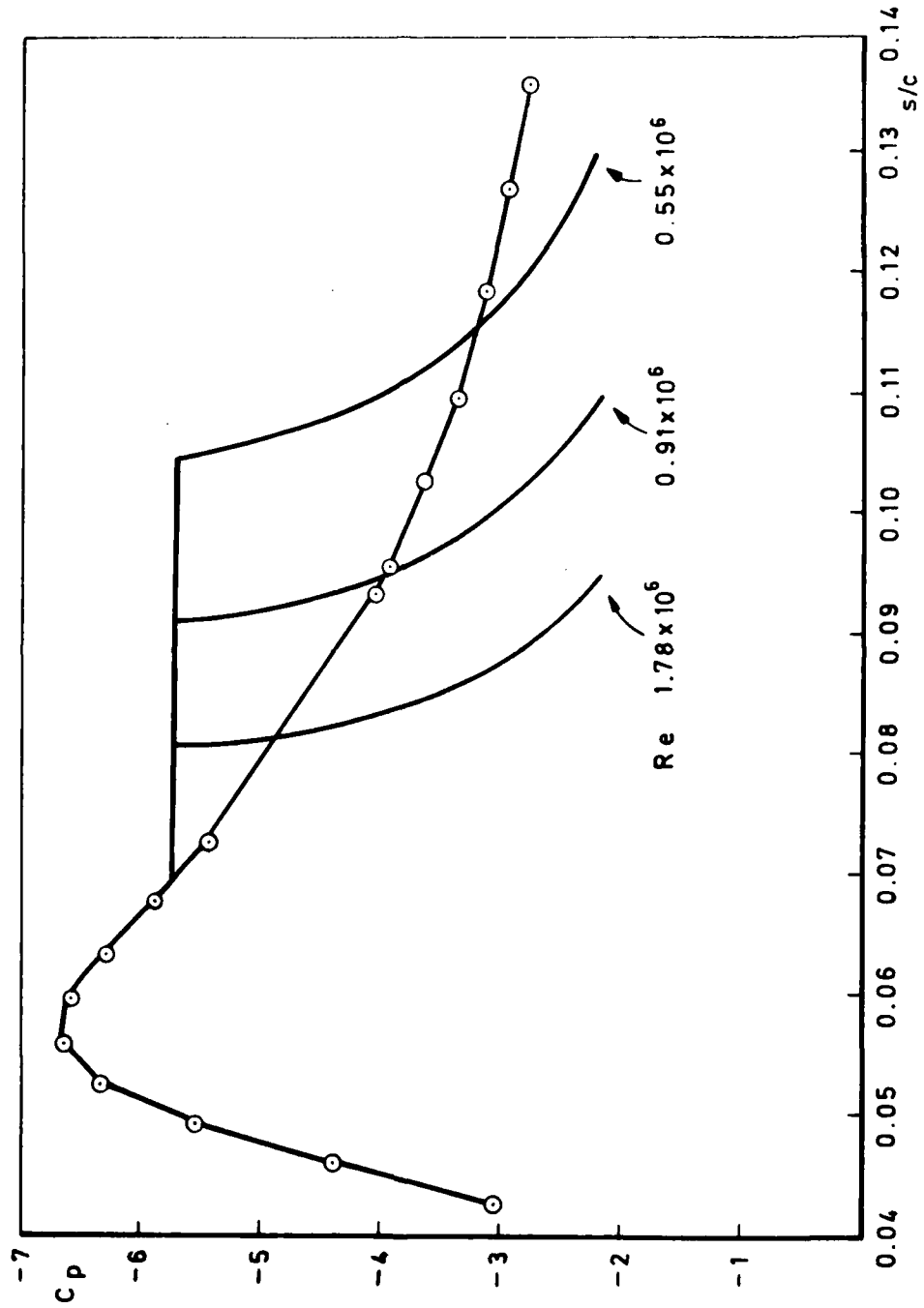


Fig 20 Pressure rise assuming equilibrium flow: RAE 100: inviscid pressure distribution $C_L = 1.305$

1. DTIC Accession Number (DTIC only) 2. Original Source (DTIC only)

5. DTIC Code for Original 6. Original Source (DTIC only)

5a. Sponsoring Agency's Code 6a. Sponsoring Agency (DTIC only) Name and Location

7. Title: The prediction of the variation of laminar separation bubbles in the design of two-dimensional high-lift airfoils

7a. (For Translations) Title in Foreign Language

7b. (For Conference Papers) Title, Place and Date of Conference

8. Author 1. Surname, Initials 9a. Author 2 9b. Author 3

11. Contract Number 12. Period 13. Project

15. Distribution statement
 (a) Controlled by - Unlimited
 (b) Special Institution (if any) -

16. Descriptors (Keywords) (Distribution statement)
 Laminar separation bubbles, High-lift airfoils,
 Laminar flow, Separation, Airfoil design

17. Abstract
 The prediction of the variation of laminar separation bubbles in the design of two-dimensional high-lift airfoils